General Disclaimer

One or more of the Following Statements may affect this Document

- This document has been reproduced from the best copy furnished by the organizational source. It is being released in the interest of making available as much information as possible.

- This document may contain data, which exceeds the sheet parameters. It was furnished in this condition by the organizational source and is the best copy available.

- This document may contain tone-on-tone or color graphs, charts and/or pictures, which have been reproduced in black and white.

- This document is paginated as submitted by the original source.

- Portions of this document are not fully legible due to the historical nature of some of the material. However, it is the best reproduction available from the original submission.

NASA TECHNICAL MEMORANDUM

NASA TM X-73689

NASA TM X-73689

INVESTIGATION OF POSSIBLE LOWER HYBRID EMISSION FROM THE NASA LEWIS BUMPY TORUS PLASMA

by R. Mallavarpu and J. R. Roth
Lewis Research Center
Cleveland, Ohio 44135

TECHNICAL PAPER presented at the
International Conference on Plasma Science
sponsored by the Institute of Electrical and Electronics Engineers
Troy, New York, May 23-25, 1977

INVESTIGATION OF POSSIBLE LOWER HYBRID EMISSION FROM THE NASA LEWIS BUMPY TORUS PLASMA

R. Mallavarpu* and J. R. Roth

National Aeronautics and Space Administration
Lewis Research Center
Cleveland, Ohio 44135

E-9224

ABSTRACT

Radio frequency (rf) emission has been detected near the lower hybrid frequency of the NASA Lewis Bumpy Torus plasma. Such emission has now been more clearly identified than in previous attempts, using a simple but more responsive detection system that consists of a spectrum analyzer and a 50 Ω miniature co-axial antenna concentrically located in a re-entrant quartz tube. The frequency shift of a broad emission peak is monitored as a function of the background pressure, electrode voltage, and the strength of the dc magnetic field. Simultaneous measurements of the average plasma density are made with a polarization diplexing microwave interferometer. The information derived from the experiment is discussed with particular reference to the following: (a) whether the emissions are dominated by atomic or molecular species of deuterium, (b) the strength of the dc magnetic field in the emitting region, (c) the geometric location of the emitting region of the plasma, (d) comparison of the lower hybrid plasma density with the average plasma density, and (e) relation of the ion spoke geometry to the lower hybrid emission.

---

*National Research Council Research Associate.

STAR Category 75

INTRODUCTION

The identification of rf emission near the lower hybrid frequency of the NASA Lewis Bumpy Torus Plasma could provide important diagnostic information and shed further light on the propagation characteristics of a lower hybrid wave through an inhomogeneous plasma contained by strong radial electric fields and an inhomogeneous toroidal magnetic field. Such emissions from the Bumpy Torus Plasma have been identified and found to occur with high amplitudes in the low pressure mode of operation with negative electrode potentials (ref. 1). Prior to reference 1, fluctuations at the lower hybrid frequency were reported by Burtis (ref. 2) who used the emission near that frequency to determine the electron density in the outer magnetosphere on the OGO-3 satellite. More recently an rf emission spectrum ranging from 300 MHz to 5 GHz was observed in low-density discharges in the Alcator (ref. 3). A strong peak at the lower end of the spectrum was identified with the ion plasma frequency. The theoretical background relating to fluctuations at the lower hybrid frequency is briefly reviewed. Diagnostic instruments are described and experimental results pertaining to the lower hybrid emission are discussed.

THEORETICAL BACKGROUND

In a theoretical investigation Stix (ref. 4) predicts that mode conversion, that is, conversion of a fast electromagnetic plasma wave into a very slow electrostatic mode (or vice versa) can lead to effective absorption or radiation of electromagnetic energy in or from a plasma. Evidence of radiation via this process is due to Landauer (ref. 5) who detected radiation at the electron cyclotron frequency with detectors placed well outside the plasma. Stix (ref. 4) has proposed that Landauer radiation could be due initially to excitation of Bernstein modes by thermal or superthermal electrons, followed in turn by propagation of this wave energy inward to the upper hybrid critical layer, mode conversion at this layer, and tunneling past the cutoff at $\omega^2 = \omega_{pe}^2$ to a receiver outside the plasma.

A similar mechanism may explain radiation at the lower hybrid frequency. Since the Lewis Bumpy Torus has ions that are preferentially heated, energetic ions could lead to excitation of the hot plasma electrostatic mode. This mode could travel towards the lower hybrid critical layer converting to a cold plasma electromagnetic mode and tunneling past the cutoff at $\omega^2 = \omega_{pi}^2$. The lower hybrid critical layer as described by the cold-warm-hot plasma theory (ref. 6) occurs at a lower density than the density corresponding to the cold plasma lower hybrid resonance given by the equation:

$$\frac{1}{\omega_{LH}^2} = \frac{1}{\omega_{pi}^2 + \omega_{ci}^2} + \frac{1}{\omega_{ce}\omega_{ci}} . \tag{1}$$

Simonutti (ref. 7), using an electrostatic approximation, has shown that the mode conversion density is, in general, lower than the density corresponding to the cold plasma lower hybrid resonance when thermal effects are taken into account.

In calculations based on the experimental results in this report the cold plasma formula given by equation (1) has been used. Since this formula does not take thermal effects into account, discrepancies could arise between the experimental data and predictions from equation (1).

DIAGNOSTIC INSTRUMENTS

The apparatus used to detect rf emissions from the plasma is shown schematically in figure 1. The detection system consists of a 1.5 m long 50 Ω miniature coaxial line, with 1 cm of the center conductor exposed at one end to act as an antenna for receiving electromagnetic radiation. The antenna is concentrically located in a reentrant quartz tube that is inserted into the vacuum tank through an airlock. The other end of the coaxial line is connected to a flexible coaxial cable by an appropriate 50 Ω adapter, and

leads to a spectrum analyzer that can scan from 1 MHz to 1.3 GHz. To minimize cable resonances and any stray rf pickup, the length of the cable circuitry is minimized and RG-214/U coaxial cables are used.

The tube-probe assembly is located in the equatorial plane of the torus in a position shown in figure 2. The tip of the probe is 9 cm from the electrode ring in sector 8 and almost in the same vertical plane as the ring. The magnetic field at the location of the probe tip is about 0.5 tesla, with B_{max} equal to 2.4 tesla.

The frequency response of the probe assembly is fairly flat from 50 MHz to 1.3 GHz. Below 50 MHz the response falls gradually until a roll-off occurs at frequencies below 10 MHz. The response of this system in the range 0-50 MHz is shown in figure 3. Even in this range, the sensitivity of this probe assembly is at least 30 db better than that of the capacitive probe cathode follower assembly which was used previously (ref. 1) in this plasma. A paired comparison of the peaks observed by the two systems under identical plasma operating conditions is shown in figure 4.

The amplitude of the rf emissions was seen to depend on the location of the coaxial antenna with respect to the plasma boundary. Figure 5 shows a series of pictures for varying locations of the probe with respect to the plasma boundary. As might be expected, the amplitude of the peak is greatest for the closest possible location of the probe to the plasma boundary.

EXPERIMENTAL RESULTS AND DISCUSSION

Frequency spectra were taken with the rf probe system previously described. Emission near the lower hybrid frequency, if present, appears as a broad amplitude peak, shown in figure 4, for a typical set of plasma parameters. Also apparent in the same photograph is a second harmonic. The amplitude of the second harmonic, although less than the fundamental, is quite significant. This anomaly occurs because the frequency response of the rf probe improves with increasing frequency in the range shown.

The broad amplitude emission peak shifts in frequency as the plasma parameters are varied. The frequency of the peak is measured as a function of the background pressure, positive or negative electrode voltages, electrode current, and the strength of the dc magnetic field. Simultaneous measurements of the average plasma density are made with a polarization diplexing microwave interferometer.

Figure 6 shows the measured rf emission frequency versus the electrode voltage for 12 positive midplane electrode rings. The dc magnetic field is held constant at a maximum magnetic field of 2.4 tesla and data is taken in the low pressure and high pressure modes of operation. The dependence of frequency on electrode voltage for both pressures is steep at low voltages but saturates at high voltages. Upon extrapolation of these curves to $V_A = 0$, it is possible to obtain a limiting value which we identify with the ion cyclotron frequency ω_{ci}. This value may be used to relate the electron number density to the emission frequency, on the assumption that the latter is the lower hybrid frequency. The validity of such a calculation will be discussed later.

Figures 7(a) and (b) show rf emission near the lower hybrid frequency as a function of the anode voltage for several dc magnetic fields in the low pressure and high pressure modes of operation, respectively. These data show that there is a proportional shift in the emitting frequency for a given change in the applied magnetic field at the same pressure and anode voltage. This implies that this emission is dependent on the applied magnetic field and hence cannot be mistaken for an emission at the ion plasma frequency, ω_{pi}.

Figure 8 shows the emission frequency measured near the lower hybrid frequency plotted against the average plasma density measured by the polarization diplexing microwave interferometer. These curves correspond to the data of figure 6. Also plotted in figure 8 is the curve given by the formula for cold plasma lower hybrid resonance for $B = 2.4$ tesla. It appears from this that emission in the high pressure mode is taking place from a region of lesser magnetic field than that of the emitting region in the low pressure mode.

Figures 9(a) and (b) show the frequency plotted as a function of the measured average number density for the low pressure and high pressure modes respectively, and the effect of varying the maximum dc magnetic field. As

expected, for a given pressure the emission frequency is a function of the dc magnetic field.

The following additional observations can be made from the data given above.

(a) The emissions near the lower hybrid frequency seem to be dominated by the highly energetic ionized species of atomic deuterium, rather than molecular deuterium. This observation is substantiated by the fact that the experimental points in figures 8, and 9(a) and (b), lie in the neighborhood of the curves described by the cold plasma lower hybrid resonance formula. The mass of ionized atomic deuterium has been used in calculations from that formula.

(b) The strength of the dc magnetic field in the emitting region is a function of the plasma density (or electrode voltage) and the background pressure, as is evident in figures 8, and 9(a) and (b). For a maximum applied magnetic field of 2.4 tesla (see fig. 8) the magnetic field in the emitting region varies from 1.5 to 2.4 tesla.

(c) An exact value of the plasma density cannot be obtained from the frequency for lower hybrid emission since the dc magnetic field in the emitting region is not known. However, it has been possible to make an estimate of B_{dc} for the low pressure mode curve of figure 6. By extrapolating the f versus V_A curve to $V_A = 0$, $\omega_{ci}/2\pi$ was determined to be 10.5 MHz. Using this value of f_{ci}, n_e was calculated from the formula for cold plasma lower hybrid resonance and plotted against $\bar{n}_e$, as shown in figure 10. The experimental points fall into two distinguishable regions. Region I represents experimental points that lie on a 45^o slope line and correspond to lower hybrid emission densities that are four times higher than the average plasma densities. Region II represents a marked departure from the 45^o line. The density calculations in this region could be erroneous for two reasons: (1) the assumed value of B_{dc} in the formula for the cold plasma lower hybrid resonance is no longer valid and (2) finite temperature effects may be significant enough to cause a departure from the density described by the cold plasma lower hybrid resonance formula.

(d) For the experimental data presented in this report, the magnetic field in the emitting region varies from 1.5 to 2.4 tesla for a maximum applied magnetic field of 2.4 tesla. This region is enclosed by contours L and T, shown in figure 11. This region is just that in which we would expect the electric field between the plasma and the coil dewars to be strongest.

(e) As shown in Region I of figure 10, the electron density in the emitting region is much higher than the average electron density. This difference in density may result from the emitting region being located within the density concentration of a rotating ion spoke.

CONCLUSIONS

Radio frequency (rf) emission near the lower hybrid frequency has been identified for 12 positive electrode operation of the bumpy torus. Important diagnostic information has been obtained from the emission frequency. The emissions appear to be dominated by atomic deuterium. Emission densities are in general higher than the average density obtained by the microwave interferometer. The emission frequency appears to be dependent on the applied magnetic field, indicating that it is not emission at the ion plasma frequency. Experimental data for the rf emission does not seem to fit the entire cold plasma lower hybrid description of the resonance. Discrepancies are evident, especially at higher densities, indicating that thermal effects may be dominant.

REFERENCES

1. J. R. Roth, and G. A. Gerdin, NASA TN D-8211 (1976).

2. W. J. Burtis, J. Geophys. Res., 78, 5515 (1973).

3. A. A. M. Oomens, et al., Phys. Rev. Lett., 36, 255, (1976).

4. T. H. Stix, Phys. Rev. Lett., 15, 878 (1965).

5. G. Landauer, in Proceedings of 5th International Conference on Ionization Phenomena in Gases, Vol. 1, p. 389 (North Holland Publ. Co., Amsterdam, 1962).

6. T. H. Stix, The Theory of Plasma Waves, p. 32 (McGraw-Hill, New York, 1962).

7. M. D. Simonutti, Physics Fluids 18, 1524, (1975).

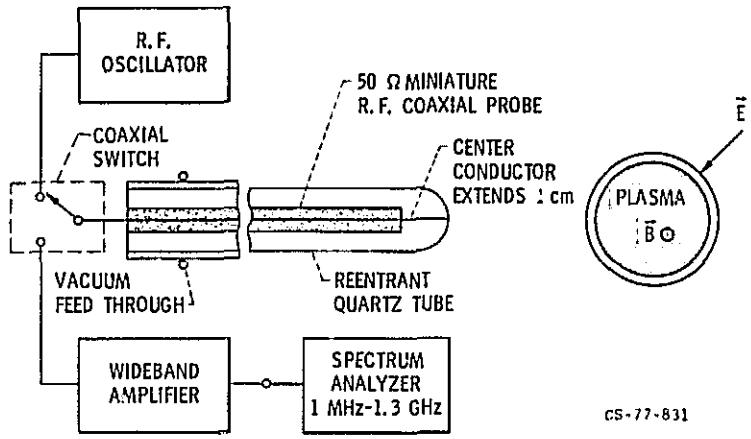

Figure 1. - Schematic of R.F. emission detecting apparatus. Tip of R.F. miniature coaxial probe is located 5-9 cms from plasma boundary. The re-entrant tube-R.F. probe assembly is approximately 1.5 m long.

Contour	Normalized magnetic field strength	Contour	Normalized magnetic field strength
A	0.050	Q	0.850
B	.100	R	.900
C	.150	S	.950
D	.200	T	1.000
E	.250	U	1.050
F	.300	V	1.100
G	.350	W	1.150
H	.400	X	1.200
I	.450	Y	1.250
J	.500	Z	1.300
K	.550	1	1.350
L	.600	2	1.400
M	.650	3	1.450
N	.700	4	1.500
O	.750	5	1.550
P	.800	6	1.600

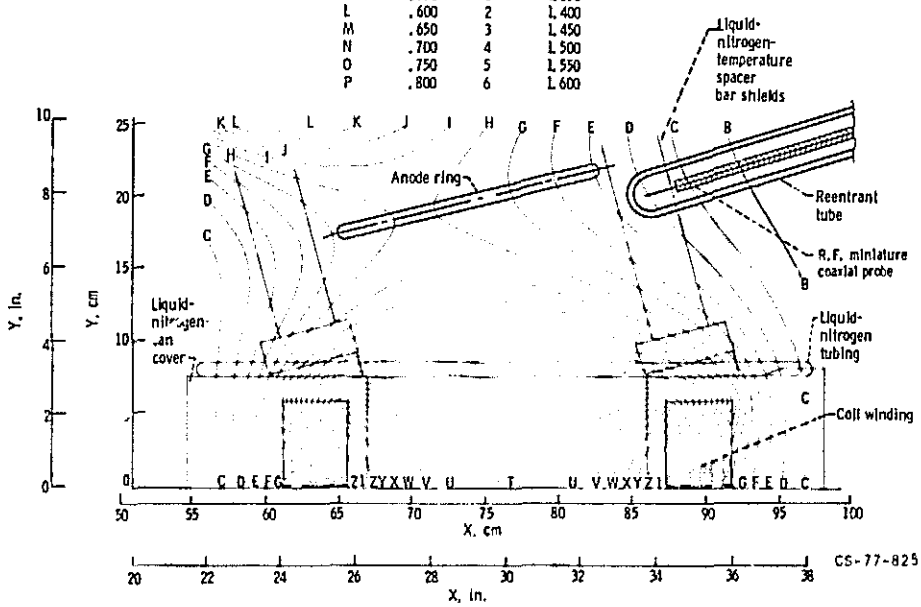

Figure 2. - Location of re-entrant tube-R.F. probe assembly with respect to the anode ring and coil dewars. Active tip of probe is 1.5 cms adjacent to the anode ring and 5-9 cms away from it. Magnetic field strength at probe tip is 20 percent of B_{max}.

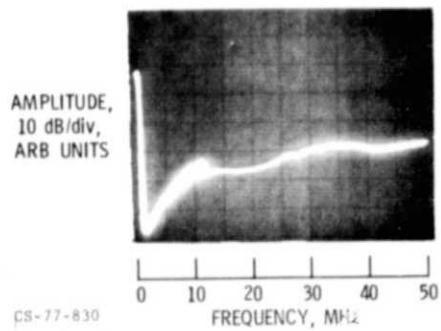

Figure 3. - Frequency response of R.F. coaxial probe.

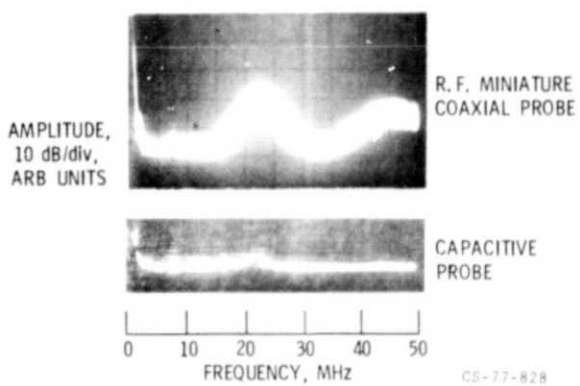

Figure 4. - Paired comparison of R.F. coaxial probe and capacitive probe responses.

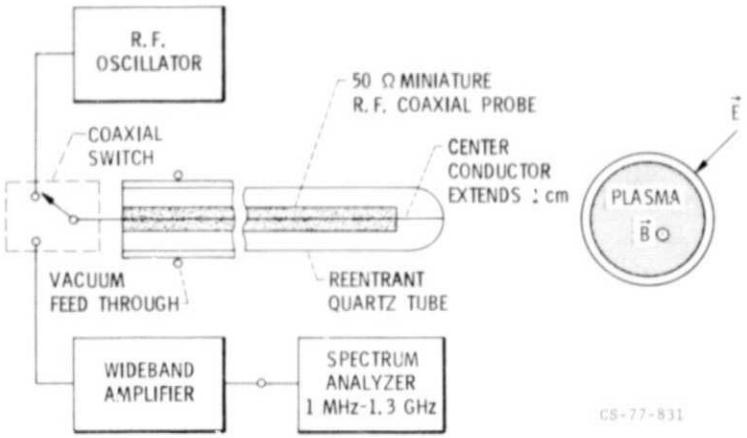

Figure 1. - Schematic of R.F. emission detecting apparatus. Tip of R.F. miniature coaxial probe is located 5-9 cms from plasma boundary. The re-entrant tube-R.F. probe assembly is approximately 1.5 m long.

Contour	Normalized magnetic field strength	Contour	Normalized magnetic field strength
A	0.050	Q	0.850
B	.100	R	.900
C	.150	S	.950
D	.200	T	1.000
E	.250	U	1.050
F	.300	V	1.100
G	.350	W	1.150
H	.400	X	1.200
I	.450	Y	1.250
J	.500	Z	1.300
K	.550	1	1.350
L	.600	2	1.400
M	.650	3	1.450
N	.700	4	1.500
O	.750	5	1.550
P	.800	6	1.600

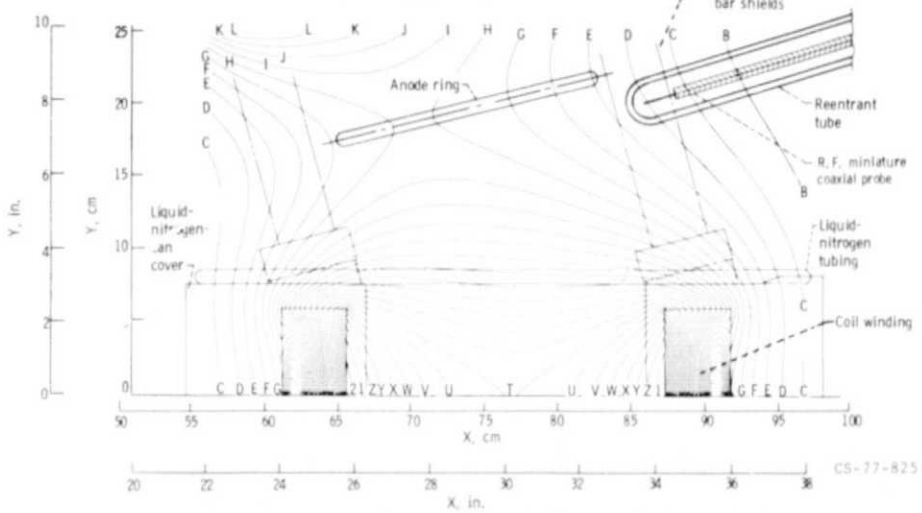

Figure 2. - Location of re-entrant tube-R.F. probe assembly with respect to the anode ring and coil dewars. Active tip of probe is 1.5 cms adjacent to the anode ring and 5-9 cms away from it. Magnetic field strength at probe tip is 20 percent of B_{max}.

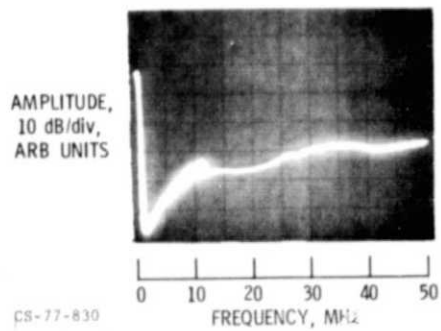

Figure 3. - Frequency response of R.F. coaxial probe.

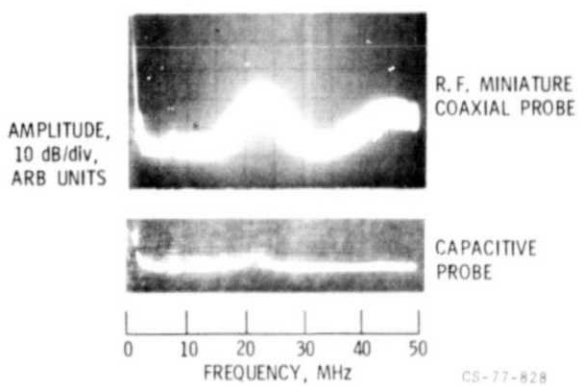

Figure 4. - Paired comparison of R.F. coaxial probe and capacitive probe responses.

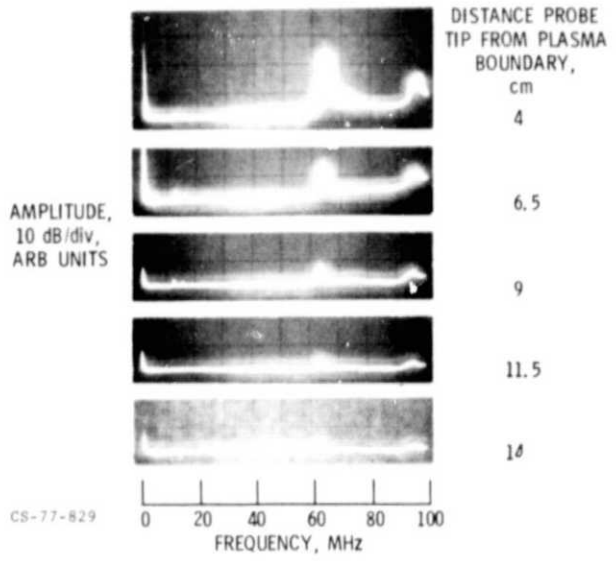

Figure 5. - Response of R.F. coaxial probe versus distance from plasma boundary.

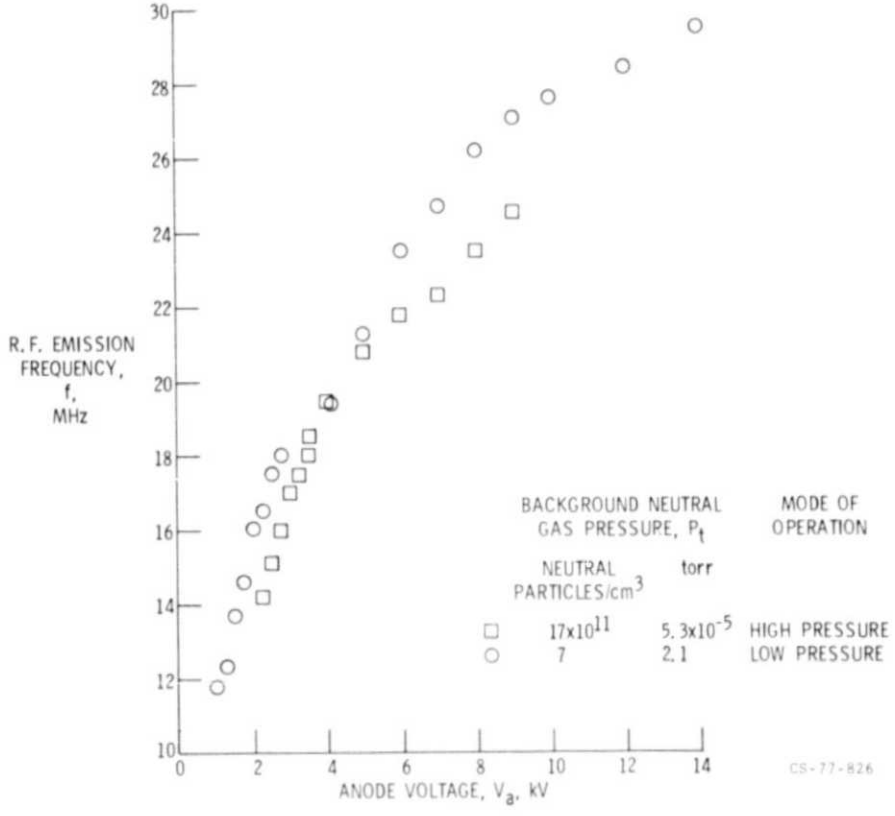

Figure 6. - Frequency of moving peaks as a function of electrode voltage for various background pressures of neutral deuterium gas. Twelve positive midplane electrode rings, maximum magnetic field strength B_{max} = 2.4 tesla.

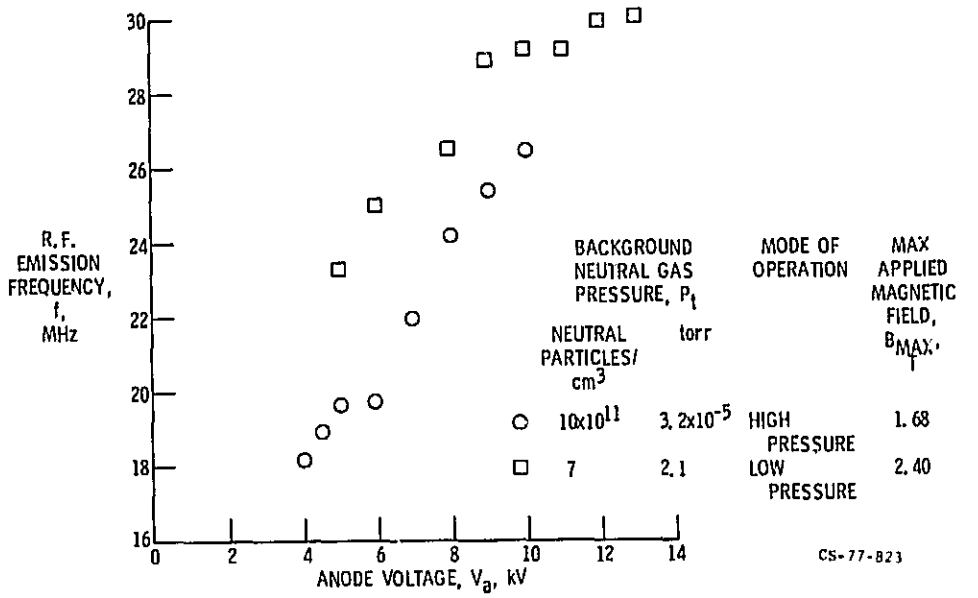

Figure 7a. - Frequency of moving peaks as a function of electrode voltage for various values of the maximum magnetic field strength. Twelve positive midplane electrode rings.

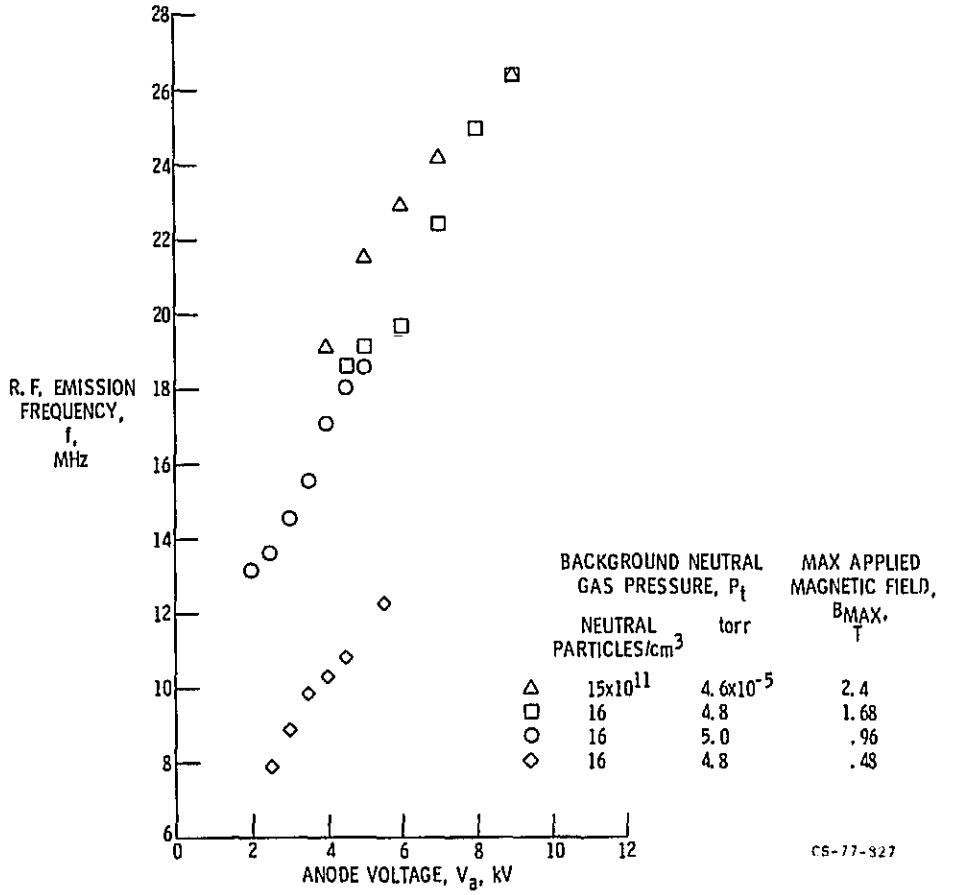

Figure 7b. - Frequency of moving peaks as a function of electrode voltage for various values of maximum magnetic field strength. Twelve positive midplane rings, high pressure mode of operation.

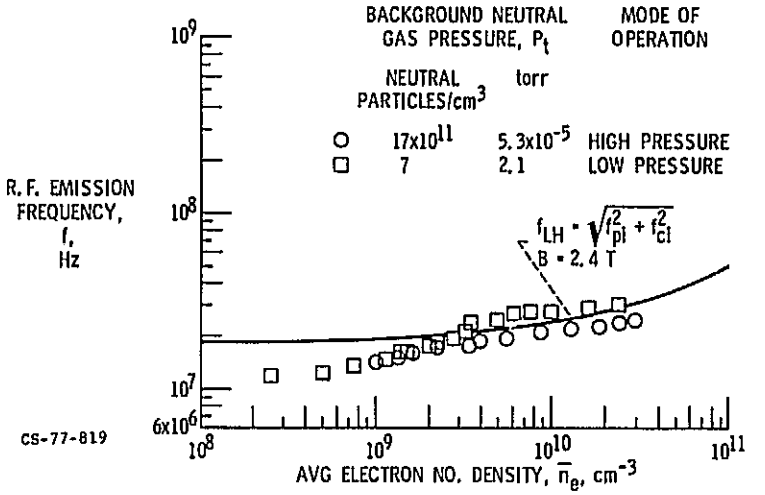

Figure 8. - Frequency of moving peaks as a function of the average electron number density as measured by the polarization diplexing microwave interferometer. Twelve positive midplane electrode rings. Maximum magnetic field strength, B_{max} = 2.4 tesla. Also shown in the figure is the curve described by the cold plasma lower hybrid resonance formula for B = 2.4 tesla.

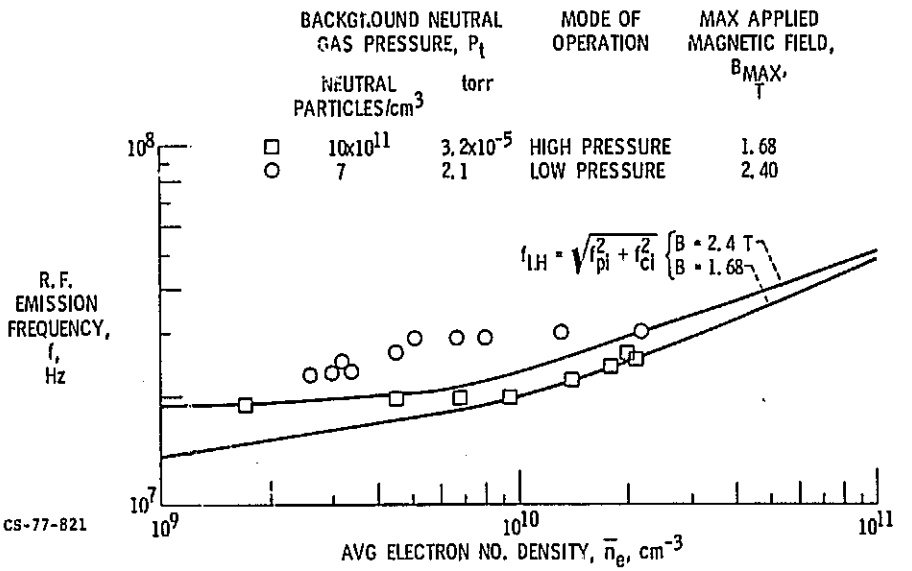

Figure 9a. - Frequency of moving peaks as a function of the average electron number density and the maximum applied magnetic field. Twelve positive midplane electrode rings. Also shown in the figure are curves described by the cold plasma lower hybrid resonance formula for B = 2.4 tesla and 1.68 tesla.

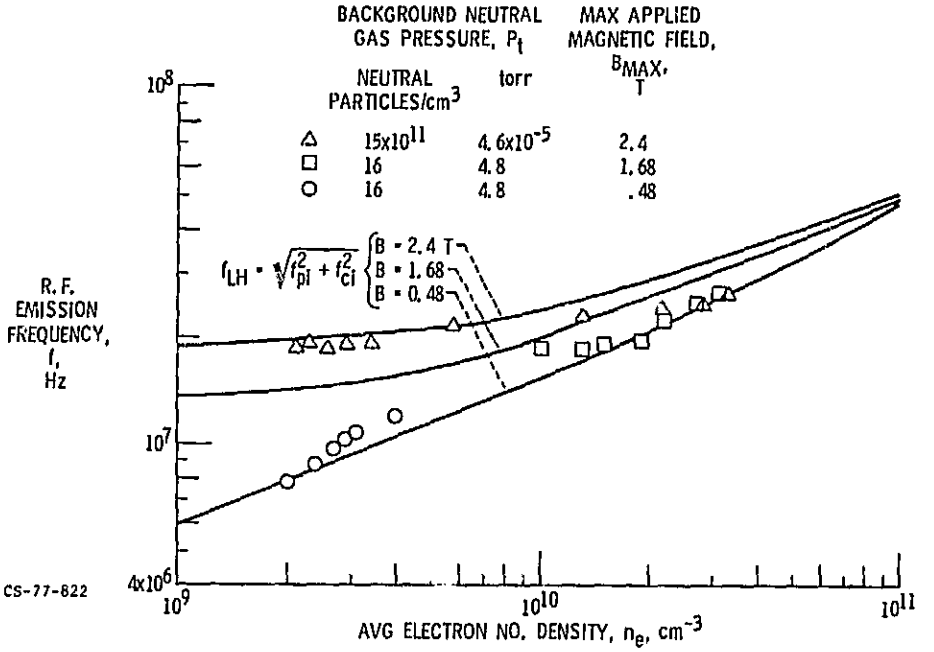

Figure 9b. - Frequency of moving peaks as a function of the average electron number density and the maximum applied magnetic field in the high pressure mode of operation. Twelve positive midplane electrode rings. Also shown in the figure are curves described by the cold plasma lower hybrid resonance formula for B = 2.4 tesla, 1.68 tesla, 0.48 tesla.

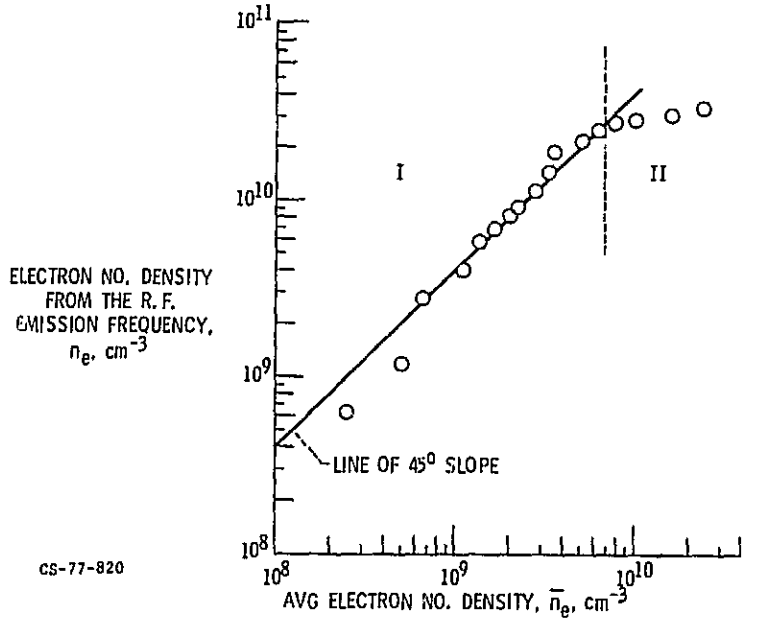

Figure 10. - Electron number density from the R.F. emission frequency versus the average electron number density in the low pressure mode of operation. Background deuterium gas pressure $p_t = 2.1 \times 10^{-5}$ torr, applied maximum magnetic field = 2.4 tesla, positive midplane electrode rings.

Contour	Normalized magnetic field strength	Contour	Normalized magnetic field strength
A	0.050	Q	0.850
B	.100	R	.900
C	.150	S	.950
D	.200	T	1.000
E	.250	U	1.050
F	.300	V	1.100
G	.350	W	1.150
H	.400	X	1.200
I	.450	Y	1.250
J	.500	Z	1.300
K	.550	1	1.350
L	.600	2	1.400
M	.650	3	1.450
N	.700	4	1.500
O	.750	5	1.550
P	.800	6	1.600

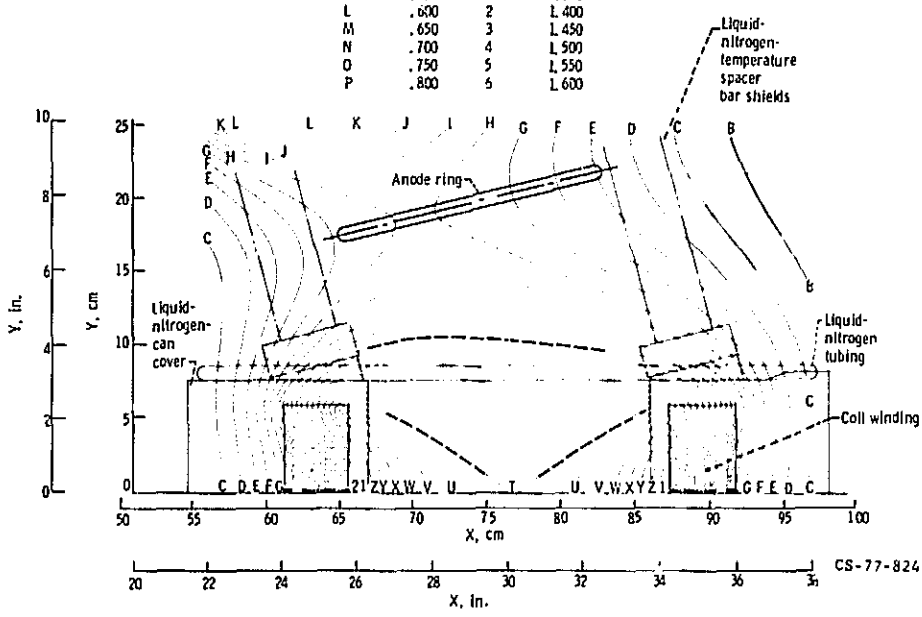

Figure 11. - Approximate geometric location of the lower hybrid emitting region. Dotted lines indicate upper and lower limit of the magnetic field strength variation in the emitting region for an applied maximum magnetic field of 2.4 tesla.